

Evaluation of optimum season selection for construction RSEI: A case study of ecological environment quality assessment in the Beijing-Tianjin-Hebei region from 2001 to 2020

Shaodong Huang¹, Yujie Li¹, Haowen Hu¹, Pengcheng Xue¹, Nina Xiong¹, and Jia Wang¹

¹Beijing Forestry University College of Forestry

March 3, 2023

Abstract

Timely and objective assessment of the optimal season for the construction of remote sensing ecological index (RSEI) is of great significance for accurate and effective assessment of ecological environment quality. We manipulated RSEI in different seasons to monitor and evaluate seasonal ecological environment quality (EEQ) variations in the Beijing-Tianjin-Hebei (JJJ) region from 2001 to 2020. First, we evaluated the image quality, and the bad observations were interpolated. Second, the seasonal RSEI was constructed by MODIS, and we compared the eigenvalues contribution rate of PC1 in seasons. Third, we assessed the temporal and spatial variations in EEQ across the same season within distinct years. Third, Moran's I was employed to evaluate the spatial autocorrelation of EEQ and the stability of mean and standard deviation of correlation between RSEI and four indicators of seasons was compared. The results showed that: 1) the PC1 component concentrates most of the characteristics of the four indicators, especially in summer (over 71%); 2) the Moran's I in the summer of 2001, 2006, 2011, 2016, and 2020 are 0.909, 0.898, 0.917, 0.921, and 0.892, respectively, which indicated that the EEQ has a strong positive spatial correlation. 3) the correlation between the four indicators and summer RSEI showed high correlation in different years, and the standard deviation of the correlation between the four indicators and RSEI fluctuated most slightly in summer, which the std of NDVI, WET, LST, and, NDBSI were 0.005, 0.052, 0.026, and 0.017, respectively. 4) Only the RSEI in summer and the VCF show spatial distribution consistency in the long time series RSEI spatial distribution of four seasons. This study explored the spatiotemporal variations of EEQ in the JJJ region at a seasonal scale, which can provide a reference for selecting the optimum season for the ecological quality monitoring of urban agglomeration in the future.

Evaluation of optimum season selection for construction RSEI: A case study of ecological environment quality assessment in the Beijing-Tianjin-Hebei region from 2001 to 2020

Shaodong Huang ^{a, b}, Yujie Li ^{a, b}, Haowen Hu ^{a, b}, Pengcheng Xue ^{a, b}, Nina Xiong ^{a, b}, Jia Wang ^{a, b, *}

^a Beijing Key Laboratory of Precision Forestry, Beijing Forestry University, Beijing 100083, China

^b Institute of GIS, RS & GPS, Beijing Forestry University, Beijing 100083, China

Abstract

Timely and objective assessment of the optimal season for the construction of remote sensing ecological index (RSEI) is of great significance for accurate and effective assessment of ecological environment quality. We manipulated RSEI in different seasons to monitor and evaluate seasonal ecological environment quality (EEQ) variations in the Beijing-Tianjin-Hebei (JJJ) region from 2001 to 2020. First, we evaluated the image quality of four seasons, and the bad observations were interpolated using the linear interpolation approach. Second, the seasonal RSEI was constructed by MODIS and its products in the years 2001, 2006, 2011, 2016, and 2020, and we compared the eigenvalues contribution rate of PC1 in different seasons. Third, we assessed the temporal and spatial variations in EEQ across the same season within distinct years. Third, Moran's I was employed to evaluate the spatial autocorrelation of EEQ, and the stability of mean and standard deviation of correlation between RSEI and four indicators of seasons was compared. Finally, the spatial distribution of Vegetation Continuous Fields (VCF) was used to compare with seasonal RSEI. The results showed that: 1) The effect of cloud/snow/ice on image quality in winter is worse than that of cloud/cloud shadow on image quality in other seasons. Additionally, the PC1 component concentrates most of the characteristics of the four indicators, especially in summer (over 71%); 2) the Moran' I in the summer of 2001, 2006, 2011, 2016, and 2020 are 0.909, 0.898, 0.917, 0.921, and 0.892, respectively, which indicated that the EEQ has a strong positive spatial correlation. 3) the correlation between the four indicators and summer RSEI showed high correlation in different years, and the standard deviation of the correlation between the four indicators and RSEI fluctuated most slightly in summer, which the std of NDVI, WET, LST, and, NDBSI were 0.005, 0.052, 0.026, and 0.017, respectively. 4) Only the RSEI in summer and the VCF show spatial distribution consistency in the long time series RSEI spatial distribution of four seasons. This study explored the spatiotemporal variations of EEQ in the JJJ region at a seasonal scale, which can provide a reference for selecting the optimum season for the ecological quality monitoring of urban agglomeration in the future.

Keywords: Optimum seasonal selection, Seasonal RSEI, JJJ region, Spatiotemporal changes, Correlation analysis

* Corresponding author. Beijing Key Laboratory of Precision Forestry, Beijing Forestry University, Beijing, 100083, China.

E-mail addresses: wangjia2009@bjfu.edu.cn (J. Wang).

40

41 1. Introduction

42 The status of ecological environment is inextricably linked to human survival (Yue et al., 2019).
43 Since reforming and opening in 1978, urbanization has accelerated dramatically and Land use and
44 Land cover (LULC) also changed significantly in China (Ji et al., 2020a), according to the National
45 Bureau of Statistics, China's urbanization rate increased from 17.92 % to 63.89% between 1978 and
46 2020.(Ji et al., 2022), with China's urbanization rate expected to reach 70% by 2030.(Tian et al.,
47 2020). Urbanization has promote the economic, social, and cultural development (Zhou et al., 2018),
48 but it also has aggravated the pressure on ecological environment quality (EEQ) and led to a series
49 of environmental issues (Airiken et al., 2022; Huang et al., 2021), such as biodiversity loss
50 (McDonald et al., 2013), desertification (Zhang et al., 2018), grassland degradation (Wen et al.,
51 2013), soil erosion (Jeong and Dorn, 2019), hydrological fluxes, and biogeochemical cycles altera-
52 tion (Kalantari et al., 2017; Schneider et al., 2015), and so forth. In areas of increasing urbanization,
53 the ecological environment has become extremely vulnerable, with a slew of ecological function
54 degradation and eco-environmental issues (Tian et al., 2020; Zang et al., 2011). It is urgent and
55 realistic to conduct timely, accurate, quick monitoring and quantitative assessment of the spatiotem-
56 poral changes in the eco-environment of the Beijing-Tianjin-Hebei (JJJ) region over a long time
57 series period.

58 With the continuous advancement of remote sensing technology, numerous satellites with vary-
59 ing temporal and spatial resolutions have been launched, and due to the benefits of regular, extensive,
60 and repetitive observations of the earth, remote sensing technology has grown in importance for
61 eco-environmental monitoring (Huang et al., 2021; Levin et al., 2020; Turner et al., 2003). Xu (2013)
62 proposed the remote sensing ecological index (RSEI) based on remote sensing technology, which
63 integrated four indicators (greenness, wetness, heat, and dryness) and was used to monitor and eval-
64 uate the EEQ of Changting county in western Fujian Province. Hereafter, due to its characteristics
65 of efficient data acquisition and objective reflection of EEQ, the RSEI has been widely used in the
66 assessment of EEQ in various scenarios, such as in cities (Ji et al., 2020a; Maity et al., 2022; Zhang
67 et al., 2021b), islands (Han et al., 2022; Liu et al., 2021), basins (Wu et al., 2020; Xiong et al., 2021;
68 Zhang et al., 2022; Zhou and Liu, 2022), oases(Gao et al., 2020), plateaus (Cao et al., 2022; Sun et
69 al., 2020), and others (Hui et al., 2021; Zhu et al., 2020).

70 Furthermore, MODIS and Landsat data are the most commonly used remote sensing data
71 sources in RSEI application scenarios. However, previous research using RSEI to monitor and eval-
72 uate EEQ based on Landsat was limited to the small region level due to cloud/cloud shadow/snow
73 contamination and the long 16-day revisit period, making it difficult to obtain all cloud-free images
74 covering a large region at a short time. (Ji et al., 2020a). Hang et al. (2020) evaluate the impact of
75 urbanization with RSEI based on Landsat-5 and Landsat-8 for Nanjing, Jiangsu Province. Xiong et
76 al. (2021) used RSEI based on Landsat-5 and Landsat-8 to assess the EEQ of Erhai lake basin,
77 Yunnan Province. Gou and Zhao (2020) used RSEI combined with Random Forest (RF) based on
78 Landsat-8 images to monitor the EEQ of Beijing, China. Liu et al. (2021) employed RSEI based on
79 Landsat-TM/OLI/TIRS to evaluate the spatiotemporal change of EEQ of Xiamen and Kinmen is-
80 lands, China. MODIS data, on the other hand, offered a cost-effective way to monitor EEQ on a
81 large scale and at regular intervals. (Xu et al., 2019). Some scholars applied time series RSEI based
82 on MODIS data to evaluate the EEQ and analysis the driving factors of the JJJ urban agglomeration
83 and China (Ji et al., 2022; Ji et al., 2020a; Ji et al., 2020b; Ji et al., 2021). Xu et al. (2019) applied

84 RSEI and change vector analysis (CVA) method to detect the eco-environment changes in Fujian
85 province based on MODIS data from 2002-2017. [Yang et al. \(2021\)](#) calculate the RSEI based on
86 MODIS to reveal the EEQ changes in the Yangtze River basin from 2001-2019. [Liao and Jiang](#)
87 [\(2020\)](#) evaluated the spatiotemporal changes of EEQ with RSEI based on MODIS from 2000-2017
88 in China. [Xia et al. \(2022\)](#) utilized MODIS data to construct RSEI and investigate the ecological
89 changes in Central Asia. In addition, RSEI is often calculated from a single image ([Gou and Zhao,](#)
90 [2020](#); [Hang et al., 2020](#); [Liu et al., 2020](#); [Xiong et al., 2021](#); [Xu et al., 2018](#); [Yuan et al., 2021](#)),
91 monthly images ([Airiken et al., 2022](#); [Xu et al., 2019](#); [Yang et al., 2021](#)), or synthesize images of
92 vegetation growing seasonal to replace annual RSEI in the previous studies ([Huang et al., 2021](#); [Ji](#)
93 [et al., 2022](#); [Ji et al., 2020a](#)).

94 In addition, acquiring the multi-temporal and high spatial-resolution images required for EEQ
95 evaluation and analysis is typically time-consuming and labor-intensive ([Huang et al., 2021](#)). These
96 issues have been resolved by the introduction of the Google Earth Engine (GEE) platform ([Zhou](#)
97 [and Liu, 2022](#)). GEE as a free and open platform for education, research, and non-profit have widely
98 applied, especially for research in the large regions even global scale due to its advantages of ena-
99 bling parallelized processing of geospatial data ([Gorelick et al., 2017](#)). Besides, GEE hosts petabytes
100 of over 40 years of remote sensing image, such as Landsat, MODIS, Sentinel, and Advanced Land
101 Observing Satellite (ALOS) data ([Gorelick et al., 2017](#); [Tamiminia et al., 2020](#)). The user-friendly
102 frontend makes it easy to work with interactive data and develop algorithms ([Mutanga and Kumar,](#)
103 [2019](#)). As a result, the GEE can serve as a cloud platform for large-scale monitoring and evaluation
104 of EEQ ([Xia et al., 2022](#)).

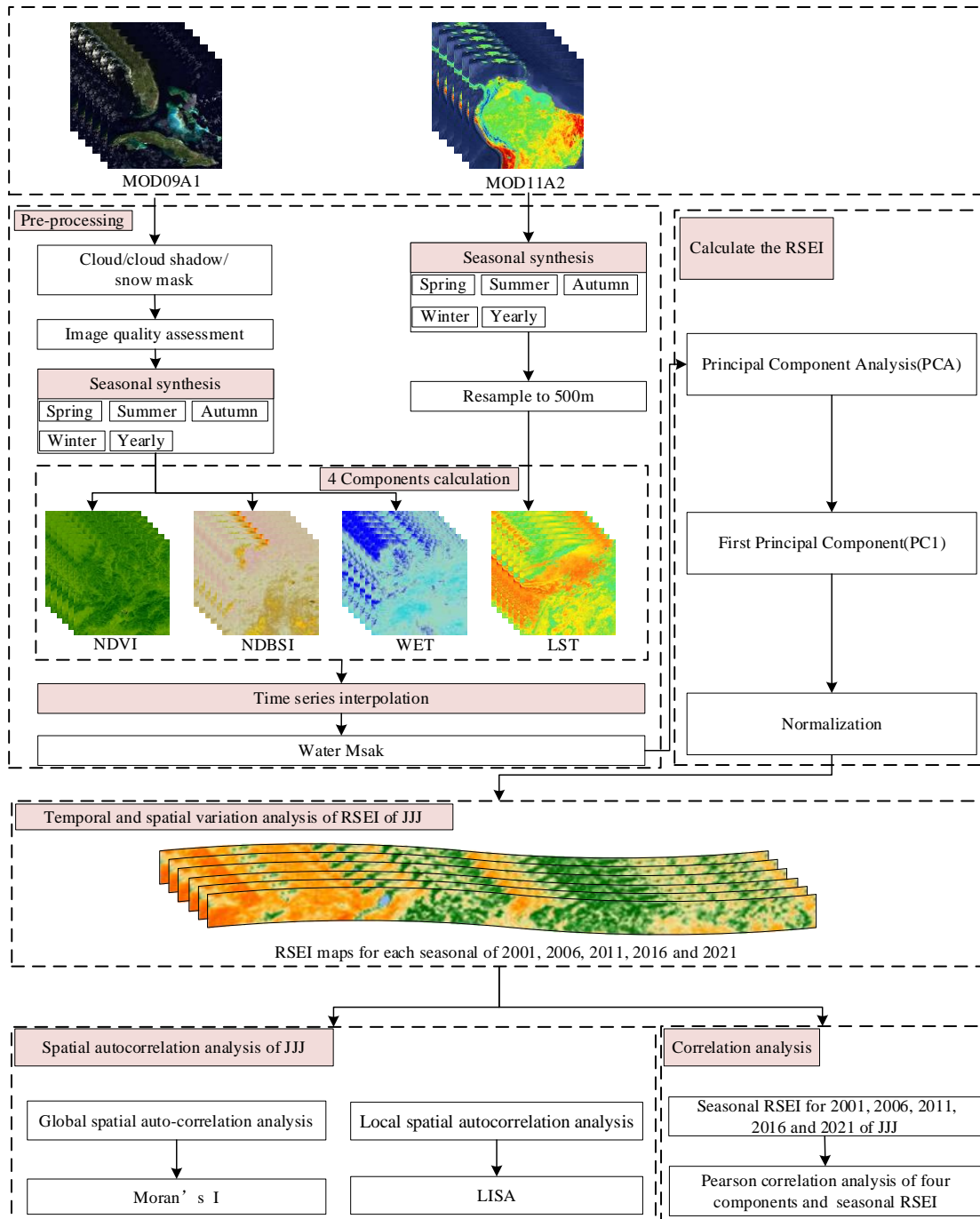
105 Till now, 272 papers on RSEI have been published both at home and abroad (including 56 in-
106 ternational papers) ([Xu and Deng, 2022](#)). However, previous published research used RSEI to mon-
107 itor and evaluate EEQ with the limitation of using a single image and composing monthly or vege-
108 tation growing images to calculate RSEI to replace the annual value, which have not explained why
109 images from the growing season or the specific period were chosen. These studies, on the other
110 hand, focus on EEQ inter-annual variation in a specific period while ignoring the seasonal RSEI
111 difference. Furthermore, RSEI is composed of four indicators: greenness, humidity, dryness, and
112 heat, and these four indicators are affected by seasonal factors such as rainfall, temperature, and
113 vegetation growth state. All previous studies, however, have suffered from the fact that the changes
114 in seasonal RSEI in different seasons over a long time series, as well as their correlation with the
115 four indicators, have not been studied.

116 Given the issues raised above, the JJJ region was chosen as the study area to monitor and eval-
117 uate the spatiotemporal changes in EEQ in different seasons using MODIS data and the GEE plat-
118 form. The goal of this study is to analysis the stability of the correlation between the four indicators
119 and seasonal RSEI, and to examine the performance of various seasonal RSEI to the JJJ ecological
120 quality assessments in order to determine the optimal season for assessing the ecological quality of
121 urban metropolitan regions.

122 **2. Materials and Methods**

123 A workflow was established for monitoring and evaluating the changes of seasonal EEQ as well
124 as comparing the difference of seasonal RSEI ([Fig. 1](#)). First, after removing the clouds/cloud shadow
125 and snow/ice pixels from the images, the linear interpolation method was used to interpolate the bad
126 observations; Second, seasonal and annual images were synthesized to calculate the RSEI for 2001,

127 2006, 2011, 2016 and 2020, respectively; Third, the spatiotemporal changes of EEQ were analyzed
 128 by Local indicator of spatial association (LISA) and Moran's index (Moran's I). Finally, we explored
 129 the correlation between different seasonal RSEI and the four indicators of RSEI.

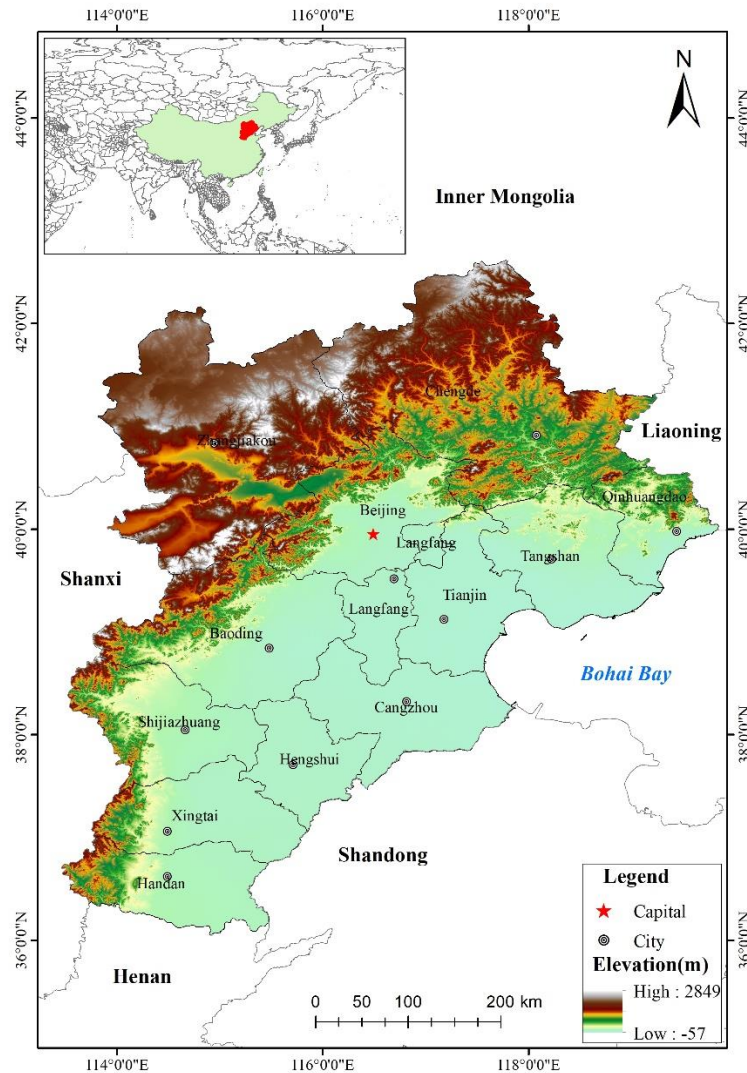


130
 131 **Fig. 1.** Workflow of the study.

132 **2.1 Study area**

133 JJJ region is in northern China (36°05' ~ 42°40'N, 113°27' ~ 119°50'E) and covers approxi-
 134 mately 2.18×10^4 km² (Ji et al., 2020a) (Fig. 2). The region contains a variety of landforms.
 135 Mountains, plateaus, and basins dominate the western and northern regions, while plains dominate
 136 the eastern and southern regions (Zhang et al., 2021a). The elevation of the region is higher in the
 137 northwest than in the southeast, and the predominate land types are construction land, forest, and

138 grassland (Liang et al., 2022). In addition, the JJJ region was consist of the municipality directly
139 under the central government of Beijing, Tianjin, and 11 cities in Hebei Province (Zhou et al., 2018).
140 The coordinated development of the JJJ region is one of the three national strategies (Li et al., 2022).
141 The JJJ region has a temperate semi-humid and semi-arid continental monsoon climate with four
142 distinct seasons and significant annual rainfall variations (Deng et al., 2021).



143
144 **Fig. 2.** Location of the Beijing-Tianjin-Hebei region.

145 *2.2 Data and preprocessing*

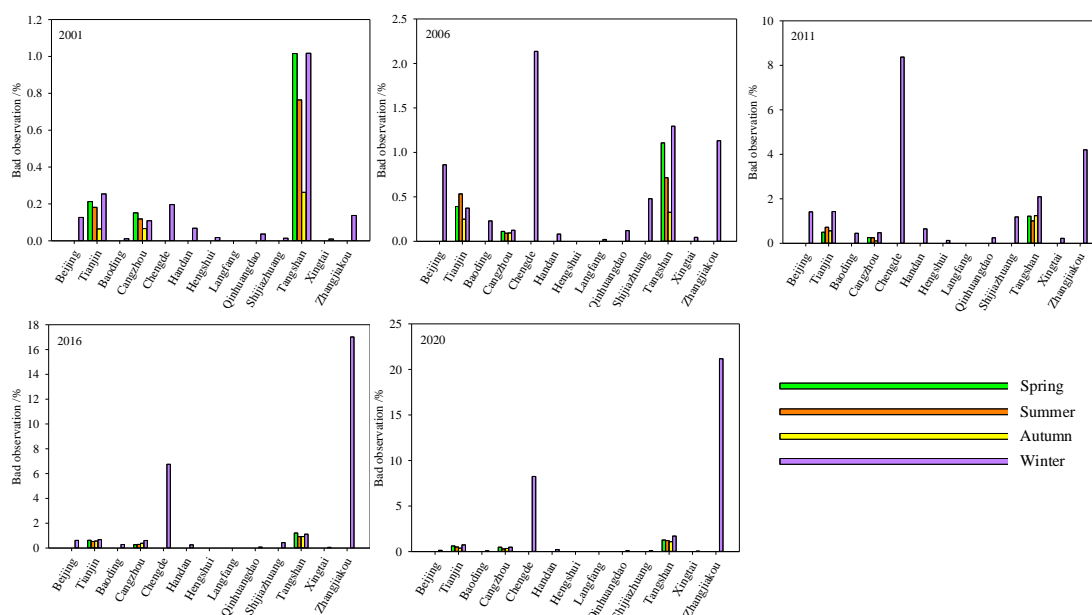
146 In this study, we employed MOD09A1 and MOD11A2 to calculate the four indicators that
147 synthesize the RSEI. The above data were pre-processed on GEE, including corrections for atmos-
148 pheric conditions such as Rayleigh scattering (Vermote et al., 2011). The MOD09A1 product pro-
149 vides an estimate of the surface spectral reflectance of Terra MODIS bands 1-7 at 500 m resolu-
150 tion (Vermote et al., 2011). The MOD11A2 product provides an average 8 days land surface tem-
151 perature (LST) at 1000m resolution (Wan et al., 2015) (Table. 1). The MOD11A2 data is
152 resampled to 500m to unify the spatial resolution of the MOD11A2 and MOD09A1 (Yang et al.,
153 2022). The images of 2001, 2006, 2011, 2016, and 2020 were synthesized based on GEE accord-
154 ing to season (Spring: 1 Mar to 31 May; Summer: 1 Jun to 31 Aug; Autumn: 1 Sep to 30 Nov;

155 Winter: 1 Dec to 28 Feb of the following year) and the annual from Jan to Dec. In addition, the
 156 Vegetation Continuous Fields (VCF) product of MOD44B, which provides the surface vegetation
 157 cover estimates globally was employed to compare with the spatial distribution of the seasonal
 158 RSEI.
 159 **Table 1**
 160 Datasets catalog introduction.

Name	Resolution	Data sources	Description
MOD09A1	500m/8 days	https://lpdaac.usgs.gov/products/mod09a1v006/	A product of surface spectral reflectance of MODIS bands 1-7
MOD11A2	1000m/8 days	https://lpdaac.usgs.gov/products/mod11a2v006/	A product of land surface temperature
MOD44B	250m/ year	https://lpdaac.usgs.gov/products/mod44bv006/	A product of a sub-pixel-level representation of surface vegetation cover estimates globally

161 *2.3 Assessment of image quality and interpolation*

162 The quality of all MOD09A1 pixels' observations was evaluated. According to the F-mask, the
 163 bad observations of clouds/cloud shadow and snow/ice were classified as NODATA (Wang et al.,
 164 2017; Zhu and Woodcock, 2012). Since the RSEI calculation in this study was based on seasonal
 165 image synthesis, it was necessary to ensure that each composite image had at least one good obser-
 166 vation pixel. The proportion of bad observations was counted in 13 cities in different seasons of
 167 2001, 2006, 2011, 2016, and 2020 respectively (Fig. 3). The bad observations were mainly con-
 168 centrated in winter, particularly in Chengde and Zhangjiakou. In 2016 and 2020, the number of
 169 pixels that had good observations was zero accounts for more than 16% and 20% in the winter
 170 season in Zhangjiakou respectively. To fill the bad observations, a linear interpolation method was
 171 employed for each time series based on GEE (Stöckli et al., 2005; Wang et al., 2010).



172

173 **Fig. 3.** Percentage of pixels with bad observations counts in the different seasons from 2001 to
 174 2020.

175 2.4 Construction of remote sensing ecological indices

176 2.4.1 Four indicators of RSEI

177 RSEI was proposed by Xu and it can quickly monitor and evaluate ecological conditions solely
178 based on remotely sensed data (Xu, 2013; Xu et al., 2018; Xu et al., 2019). The four most important
179 indicators for the human intuitive perception of the excellent or poor quality of ecological conditions
180 were integrated using Principal Component Analysis (PCA). (Xu, 2013). Greenness, moisture, heat,
181 and dryness are the four indicators, which represent vegetation, soil moisture, temperature, and built
182 lands/bare areas, respectively. (Hu and Xu, 2018; Xu et al., 2019). RSEI can be expressed as:

$$183 \quad RSEI = f(\text{Greenness}, \text{Moisture}, \text{Dryness}, \text{Heat}) \quad (1)$$

184 Greenness denoted with NDVI can be expressed as (Rousel et al., 1973):

$$185 \quad NDVI = (\rho_{NIR} - \rho_{Red}) / (\rho_{NIR} + \rho_{Red}) \quad (2)$$

186 Wet as a component derived from Tasseled Cap Transformation (TCT) represents the moisture
187 component of RSEI. The wet component based on MOD09A1 can be calculated as (Lobser and
188 Cohen, 2007):

$$189 \quad \text{Wet} = 0.1147\rho_{Red} + 0.2489\rho_{NIR1} + 0.2408\rho_{Blue} + 0.3132\rho_{Green} - 0.3122\rho_{NIR2} - \\ 190 \quad 0.6416\rho_{SWIR1} - 0.5087\rho_{SWIR2} \quad (3)$$

191 NDBSI is made up of the index-based built-up index (IBI) and the soil index (SI) which rep-
192 resents built-up lands and bare areas according to Xu (Hu and Xu, 2018), and it can be expressed
193 as:

$$194 \quad NDBSI = (IBI + SI) / 2 \quad (4)$$

$$195 \quad IBI = \frac{2\rho_{SWIR1} / (\rho_{SWIR1} + \rho_{NIR}) - [\rho_{NIR} / (\rho_{NIR} + \rho_{Red}) + \rho_{Green} / (\rho_{Green} + \rho_{SWIR1})]}{2\rho_{SWIR1} / (\rho_{SWIR1} + \rho_{NIR}) + [\rho_{NIR} / (\rho_{NIR} + \rho_{Red}) + \rho_{Green} / (\rho_{Green} + \rho_{SWIR1})]} \quad (5)$$

$$196 \quad SI = [(\rho_{SWIR1} + \rho_{Red}) - (\rho_{NIR} + \rho_{Blue})] / [(\rho_{SWIR1} + \rho_{Red}) + (\rho_{NIR} + \rho_{Blue})] \quad (6)$$

197 Heat is represented by the LST of MOD11A2 in this study. LST is an important indicator used
198 to investigate ecological processes and climate change (Liao et al., 2022; Xu et al., 2019).

199 2.4.2. Integration of the four Indicators

200 PCA was selected to integrate the four indicators because it is a multi-dimensional data com-
201 pression technique that chooses a few important variables through an orthogonal linear transfor-
202 mation of multiple variables. The advantage of PCA is that the weight of each indicators is deter-
203 mined automatically and objectively based on the character of the data and the contribution rate of
204 each index to each principal component (Xu, 2013). The first component of PCA (PC1) explains
205 more than 40.157% of the total variation of the dataset, especially in summer (more than 71%)
206 (Table. 2). The contribution of each indicator to RSEI is weighted by its loading to PC1 (Xu et al.,
207 2018). RSEI can be expressed as:

$$208 \quad RSEI = PC1[f(NDVI, WET, LST, NDBSI)] \quad (7)$$

209 On the one hand, indicators need to be normalized to [0, 1] before PCA due to the dimensions
210 of the four indicators is different. On the other hand, the RSEI calculated from Eq. (7) has low values
211 for representing excellent ecological conditions and high values for negative ones (Xu et al., 2019).
212 For high RSEI values to represent ecologically eligible and low values to represent poor ones, PCA1
213 needs to be subtracted from one to obtain the initial $RSEI_0$ (Xu et al., 2019).

$$214 \quad RSEI_0 = 1 - [PC1[f(NDVI, WET, LST, NDBSI)]] \quad (8)$$

215 To facilitate the measurement and comparison of indicators, $RSEI_0$ also needs to be normalized

216 to [0, 1] (Xu, 2013):

$$217 \quad RSEI = (RSEI_0 - RSEI_{0,min}) / (RSEI_{0,max} - RSEI_{0,min}) \quad (9)$$

218 The RSEI calculated by Eq (9) is the final RSEI in this study, and the lower the RSEI value is,
 219 the poor the ecological condition is, while the higher the value represent the better (Xu, 2013). The
 220 RSEI is divided into 5 grades at equal intervals, representing poor, fair and moderate, good, and
 221 excellent ecological environment, respectively (Wang et al., 2016; Xu et al., 2019).

222 **Table 2.**

223 PCA1 of four indicators in different seasons.

Year	Index	PCA1				
		Spring	Summer	Autumn	Winter	Yearly
2001	NDVI	0.552	0.564	0.551	0.097	0.525
	WET	0.487	0.372	0.515	0.261	0.511
	NDBSI	-0.630	-0.594	-0.649	-0.533	-0.575
	LST	-0.247	-0.437	-0.013	-0.799	-0.363
	Eigenvalues	0.115	0.156	0.102	0.090	0.100
	Eigenvalues contribution rate (%)	64.335	80.669	56.571	46.363	54.907
2006	NDVI	0.541	0.586	0.541	0.192	0.542
	WET	0.496	0.318	0.522	0.316	0.517
	NDBSI	-0.669	-0.559	-0.640	-0.554	-0.535
	LST	-0.118	-0.493	-0.159	-0.746	-0.391
	Eigenvalues	0.102	0.163	0.100	0.073	0.093
	Eigenvalues contribution rate (%)	57.194	78.675	53.942	40.157	49.247
2011	NDVI	0.601	0.575	0.574	0.021	0.538
	WET	0.507	0.275	0.466	0.032	0.451
	NDBSI	-0.600	-0.567	-0.672	-0.317	-0.488
	LST	-0.120	-0.521	-0.036	-0.947	-0.519
	Eigenvalues	0.105	0.144	0.110	0.085	0.113
	Eigenvalues contribution rate (%)	57.515	74.890	55.173	42.818	59.426
2016	NDVI	0.613	0.586	0.600	0.287	0.559
	WET	0.481	0.315	0.486	0.544	0.394
	NDBSI	-0.625	-0.567	-0.566	-0.438	-0.500
	LST	-0.040	-0.486	-0.288	-0.656	-0.531
	Eigenvalues	0.115	0.139	0.100	0.083	0.120
	Eigenvalues contribution rate (%)	58.341	78.255	51.548	43.990	63.228
2020	NDVI	0.606	0.582	0.605	0.189	0.644
	WET	0.509	0.325	0.531	0.547	0.474
	NDBSI	-0.609	-0.552	-0.583	-0.177	-0.562
	LST	-0.049	-0.501	-0.106	-0.796	-0.210
	Eigenvalues	0.120	0.125	0.093	0.079	0.108
	Eigenvalues contribution rate (%)	60.707	71.297	50.087	45.208	55.982

224

225 2.4.3. *Detection of ecological condition changes in the same season of different years*

226 To reveal the dynamic change of EEQ in the same season of different years, the difference in

227 RSEI levels was calculated in 5 periods (2001 to 2006, 2006 to 2011, 2011 to 2016, 2016 to 2021,
 228 and 2001 to 2020). For each pixel in the study area, we defined the score from 1 to 5 corresponding
 229 to the five ecological condition levels from poor to excellent, respectively. The difference in EEQ
 230 score between years ranged from -5 to +5. When the score is positive (1, 2, 3, 4, 5) it indicates that
 231 the EEQ has improved; when the score is 0 represented there has no change, and while the score is
 232 negative (-1, -2, -3, -4, -5) represented the EEQ has de graded. In addition, a lower score indicates
 233 a more serious ecological degradation, whereas a higher score indicates a better ecological environ-
 234 ment.

235 2.4.4. Spatial autocorrelation analysis

236 Moran's I and LISA are often used to analyze the spatial autocorrelation of EEQ (Jing et al.,
 237 2020; Xiong et al., 2021). Moran's I reflect the correlation between the neighbouring units (the
 238 pixels of 500m×500m) of geospatial space, and a value closer to 1, the stronger the correlation
 239 between units. Therefore, we utilized Moran's I to verify the correlation between the RSEI units in
 240 this study, which can be expressed as (Gong et al., 2014):

$$241 \text{Globalmoran's } I = \frac{\sum_{i=1}^n \sum_{j=1}^m W_{ij} (x_i - \bar{x})(x_j - \bar{x})}{S^2 \sum_{i=1}^n \sum_{j=1}^m W_{ij}} \quad (10)$$

$$242 S^2 = \frac{\sum_{i=1}^n (x_i - \bar{x})^2}{n} \quad (11)$$

243 where n is the grids in this study area; $i = 1, 2, 3 \dots, n$; $j = 1, 2, 3 \dots, m$. x_i is the RSEI value
 244 of the location of i ; \bar{x} represent the average RSEI values of all units in this study area; S^2 is the
 245 spatial units variance; W_{ij} is the weight matrix which can represent the relationship of spatial units.
 246 Moran's I values range from -1 to 1, with a value close to 1 indicating that the RSEI of spatially
 247 adjacent units is positively correlated and a value close to -1 indicating that it is negatively correlated.
 248 LISA index as an important index to analyze local spatial autocorrelation due to it can calculate the
 249 value of Moran's I at each spatial unit. Therefore it is to (Anselin, 1995). In this study, LISA was
 250 used to analyze the correlation of EEQ in each unit, the equation as follows (Gong et al., 2014;
 251 Xiong et al., 2021):

$$252 \text{Localmoran's } I = \frac{[(x_i - \bar{x})/S^2] \sum_{j=1}^m W_{ij} (x_j - \bar{x})}{S^2} \quad (12)$$

253 Where positive I indicates that adjacent space units have similar values (both high or both low),
 254 whereas negative I indicates that adjacent units have large value differences.

255 2.4.5. Pearson's correlation analysis

256 For the terrestrial ecosystem, its EEQ may be determined by the four indicators of RSEI (Yuan
 257 et al., 2021), but the effects of these indicators on seasonal RSEI are unclear. In order to analyze
 258 which indicator influences EEQ in different seasons in this study area, the Pearson correlation anal-
 259 ysis method was conducted for seasonal RSEI and the four indicators. The function can be calcu-
 260 lated as (Ahlgren et al., 2003):

$$261 \rho = \frac{\sum_{i=1}^N (x_i - \bar{x})(y_i - \bar{y})}{\sqrt{\sum_{i=1}^N (x_i - \bar{x})^2 \sum_{i=1}^N (y_i - \bar{y})^2}} \quad (13)$$

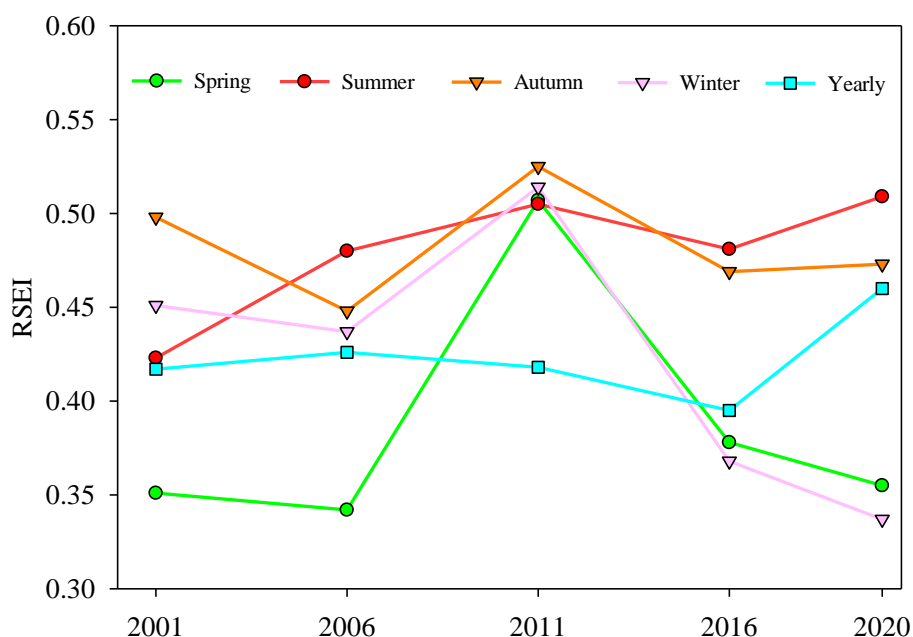
262 Where ρ denotes Pearson's correlation coefficient. When ρ is close to 0, the two variables are
 263 not correlated; when ρ is close to -1 or 1, a strong correlation between the two variables.; N is the
 264 number of spatial units; x_i and y_i denote the values of variables and RSEI of its units respectively;
 265 \bar{x} denotes the mean of the variables; \bar{y} represents the mean value of RSEI.

266 3. Results

267 3.1 Spatiotemporal changes of seasonal EEQ

268 Most the four indicators' characteristic information is concentrated on PC1. However, the con-
 269 tribution rate varies by season, with summer having a significantly higher eigenvalues contribution
 270 rate (more than 71%) than the other three seasons (Table. 2). This may be explained by Xu (2013),
 271 who states that vegetation greenness is a key factor for RSEI (Xu and Deng, 2022), therefore the
 272 eigenvalues contribution rate of PC1 of vegetation growing season is higher.

273 The variation of the seasonal RSEI mean values was depicted in Fig. 4. The graph showed that
 274 RSEI showed different trends in different seasons under the long time series. Therefore, different
 275 seasons to construct RSEI will lead to significant differences in the assessment of ecological quality.
 276 The RSEI in summer are 0.423, 0.480, 0.505, 0.481, and 0.509, respectively, showing a trend of
 277 rising, declining, and rising.

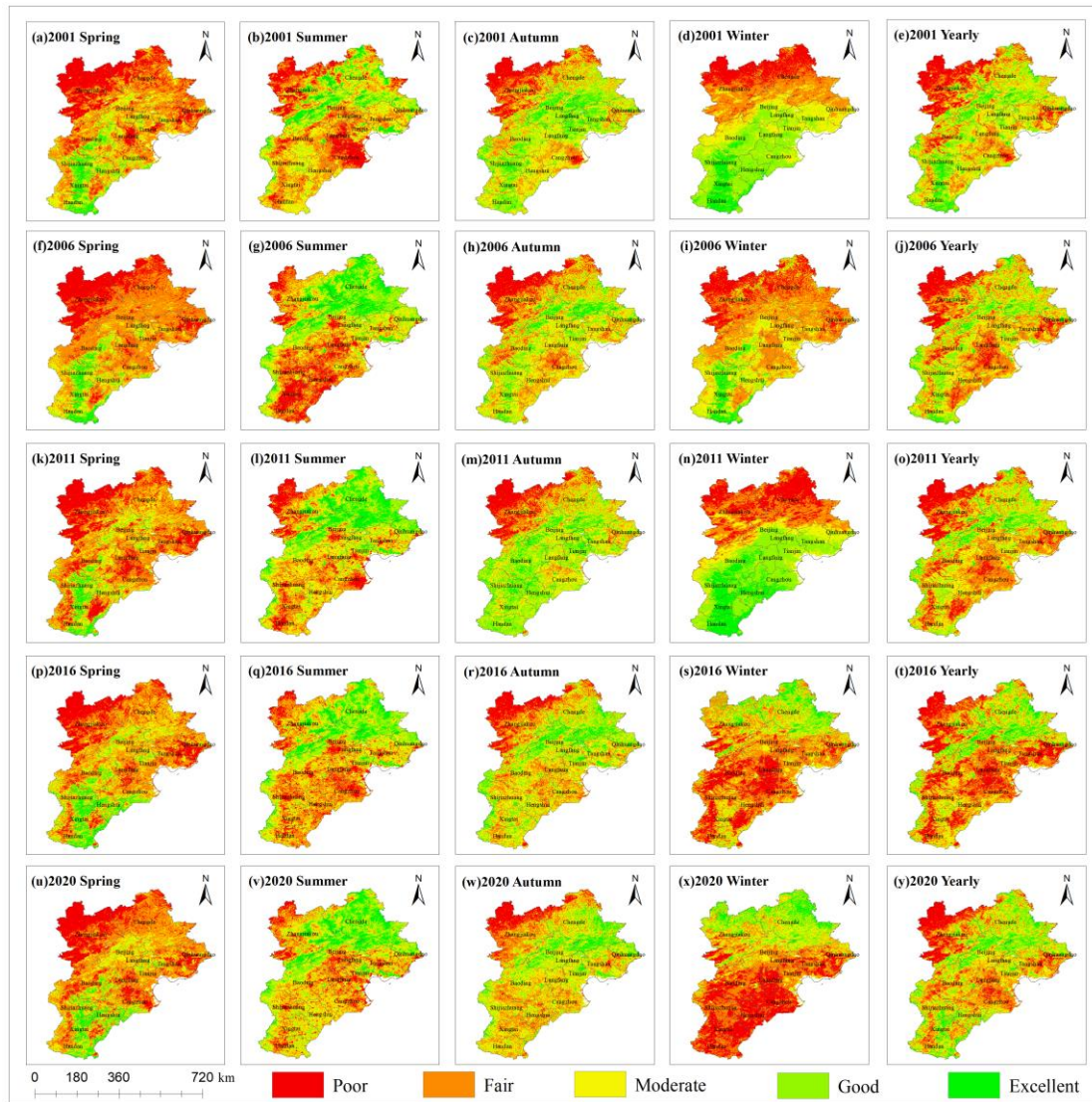


278

279 **Fig. 4.** The variation of the seasonal RSEI in the JJJ region from 2001 to 2020.

280

281 In addition, the spatial distribution of RSEI based on seasonal images also varies greatly (Fig.
 282 5). Except for the southern part of the study area, the ecological quality was poor in other regions
 283 in spring (Fig. 5a, f, k, p, u), and the ecological quality was better in northeast, but worse in north-
 284 west and south in summer (Fig. 5b, g, l, q, v). In autumn, the ecological quality of northwest JJJ is
 285 poor while that of other regions is better (Fig. 5c, h, m, r, w). The spatial distribution of RSEI in
 286 winter was different in terms of inter-annual variation, and the ecological quality was better in the
 287 south of JJJ region in the first three years while worse in the second two years (Fig. 5d, i, n, s, x).
 288 However, the spatial distribution of RSEI throughout the year is consistent with that in summer (Fig.
 5e, j, o, t, y).



289

290 **Fig. 5.** Spatial-temporal distribution of EEQ of the JJJ region in different seasons from 2001 – 2020.

291

3.2 Dynamic change analysis of EEQ

292

The spatiotemporal change of EEQ in the same season of different years and scores are shown in Fig. 6 and listed in Table 3. In fact, the scores are mainly concentrated on -1, 0, and 1. In addition, compared with the pixels with the changes, the pixels with unchanged of EEQ accounted for the largest proportion in spring (Fig. 6a, f, k, p, u), summer (Fig. 6b, g, l, q, v), autumn (Fig. 6c, h, m, r, w), and yearly (Fig. 6e, j, o, t, y). Except in winter (Fig. 6d, i, n, s, x), the proportion of pixels with scores of -4, -3, +3, or +4 does not exceed 8% respectively. It proves that despite ecological quality assessment at five-year intervals, ecological changes are not significant. No matter which season, however, the change of ecological quality will not continue to get better or worse, there is always a trend of fluctuation under a long time series. The spatiotemporal changes of EEQ in summer, for example, in the south of the study area was first degraded from 2001 to 2006 (Fig. 6b), then improved from 2006 to 2011 (Fig. 6g), and began to degraded from 2011 to 2016 (Fig. 6l), then increase again from 2016 to 2020 (Fig. 6q). However, although the ecological quality fluctuated in the past 20 years, the ecological quality of the study area showed a trend of improvement (Fig. 6v).

305

Table 3

RSEI levels change in the same seasons from 2001 to 2020.

Periods	Scores	Spring	Summer	Autumn	Winter	Yearly
		Pct/%	Pct/%	Pct/%	Pct/%	Pct/%
2001 to 2006	+4	0.00	0.80	0.00	0.00	0.00
	+3	0.06	6.44	0.21	0.12	0.09
	+2	1.14	14.27	3.69	11.25	3.04
	+1	19.69	27.45	29.20	41.03	28.03
	0	68.78	36.11	53.40	37.26	55.71
	-1	10.11	12.34	12.55	8.69	12.51
	-2	0.21	2.38	0.92	1.46	0.58
	-3	0.01	0.21	0.03	0.18	0.02
	-4	0.00	0.00	0.00	0.01	0.00
	+4	0.00	0.00	0.00	0.03	0.00
2006 to 2011	+3	0.03	0.03	0.02	0.50	0.02
	+2	0.92	1.22	0.75	2.75	0.85
	+1	16.19	17.01	11.95	11.44	18.32
	0	62.45	54.65	49.16	29.81	64.40
	-1	19.17	22.13	30.36	33.43	16.05
	-2	1.18	4.57	7.11	20.50	0.35
	-3	0.05	0.39	0.62	1.54	0.01
	-4	0.00	0.00	0.03	0.01	0.00
	+4	0.00	0.00	0.04	2.19	0.00
	+3	0.03	0.12	0.80	19.79	0.04
2011 to 2016	+2	0.35	2.11	7.31	23.31	1.33
	+1	8.95	25.30	26.64	12.88	26.49
	0	64.80	58.08	44.80	10.49	57.84
	-1	22.88	13.24	18.45	11.55	13.85
	-2	2.68	1.09	1.87	9.70	0.44
	-3	0.28	0.06	0.09	6.78	0.01
	-4	0.03	0.00	0.00	3.31	0.00
	+4	0.03	0.00	0.02	0.04	0.00
	+3	0.21	0.03	0.22	0.34	0.23
	+2	1.49	0.54	2.61	3.97	9.19
2016 to 2020	+1	21.34	11.98	20.91	20.67	53.04
	0	67.22	61.43	54.66	57.45	33.45
	-1	9.29	23.58	19.75	14.45	3.93
	-2	0.39	2.31	1.71	2.08	0.17
	-3	0.03	0.14	0.10	0.94	0.01
	-4	0.00	0.00	0.01	0.06	0.00
	+4	0.04	0.11	0.02	3.30	0.01
	+3	0.56	2.04	0.87	21.47	0.41
	+2	3.29	13.49	7.45	19.54	4.39
	+1	17.62	32.25	24.32	13.26	22.30
2001 to 2020	0	58.60	36.64	43.33	9.81	49.40
	-1	17.58	12.34	20.77	11.78	21.10
	-2	2.02	2.72	3.09	10.21	2.29
	-3	0.29	0.40	0.15	7.15	0.10
	-4	0.00	0.00	0.00	0.00	0.00

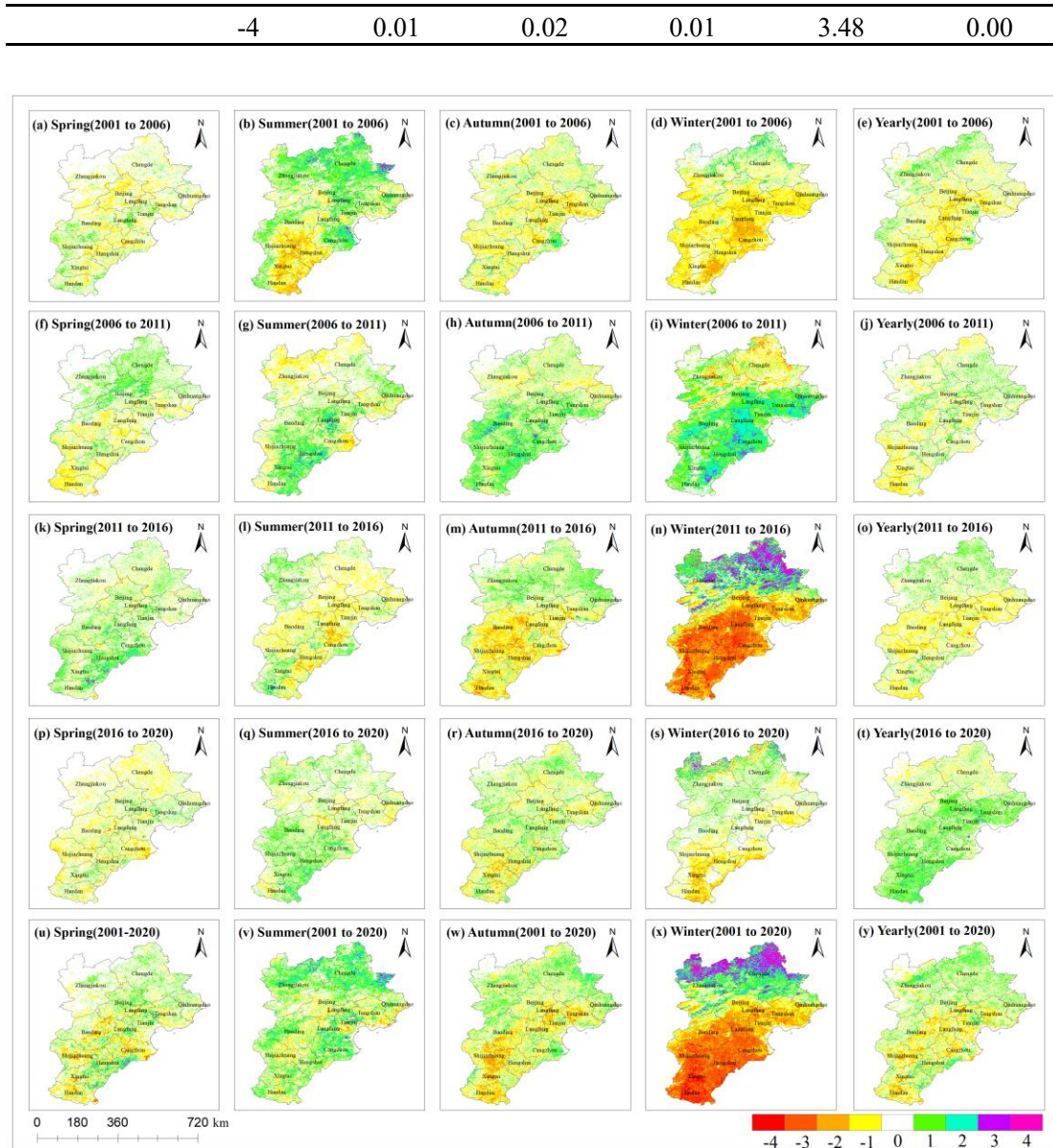


Fig. 6. Spatial-temporal distribution of RSEI change scores.

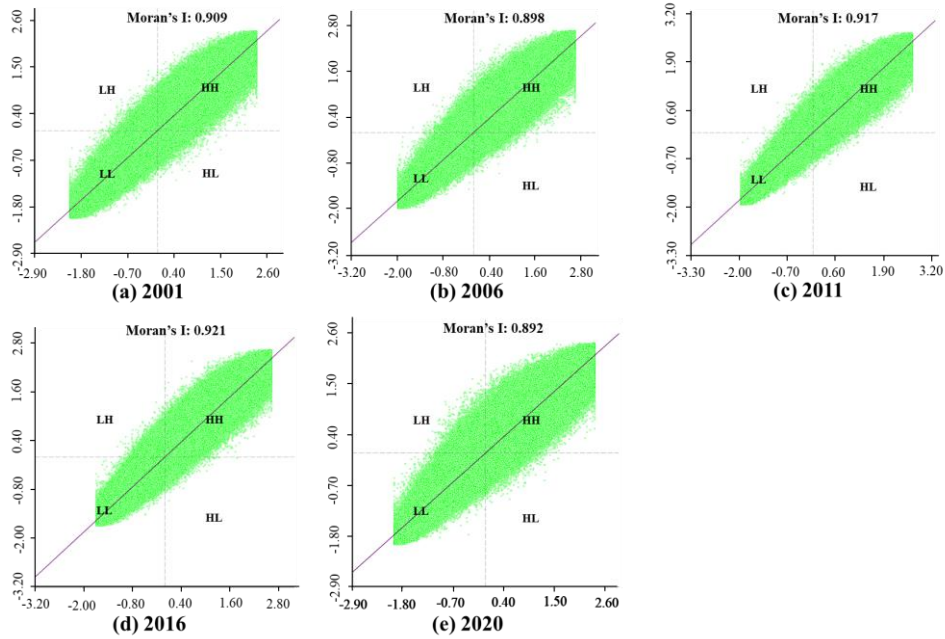
309

310

311 3.3 Spatial autocorrelation analysis of EEQ

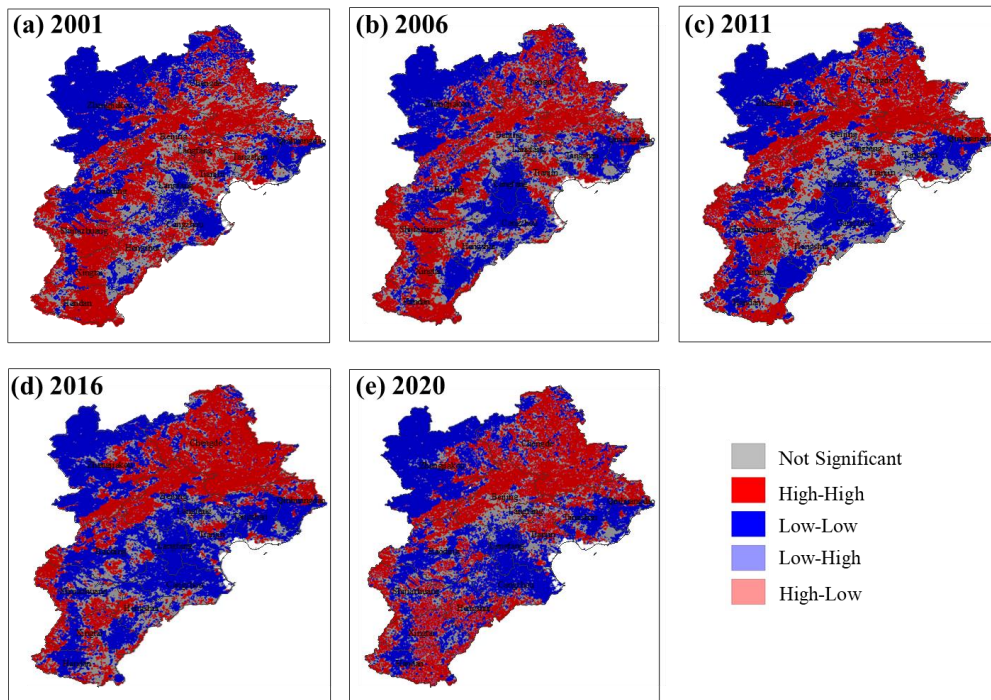
312 In order to explore whether the spatial adjacent of RSEI has a certain correlation, we plotted the
 313 Moran' I scatter plots for summer in 2001, 2006, 2011, 2016, and 2020 shown in Fig. 7. The first
 314 and third quadrants are where the scatter points are most concentrated, and the Moran' I values are
 315 0.909, 0.898, 0.917, 0.921, and 0.892, indicating that the spatial correlation of EEQ is strong posi-
 316 tive. In other words, the spatial distribution of EEQ showed a characteristic of clustering.

317 The spatial clustering is shown in Fig. 8 in which the H-H clustering area in the northeast like
 318 Chengde, while L-L clustering is in the northwest in these years. From 2001 to 2016, the L-L clus-
 319 tering continuously increased in the south of this study area like Shijiazhuang, Xingtai, and Handan.
 320 Besides, the L-L clustering area gradually expanded in Cangzhou and Langfang from 2001 to 2020.
 321 The distribution of Not insignificant regions was scattered, and the L-H and H-L regions were al-
 322 most absent.



323
324

Fig. 7. Moran'I plots distribution of RSEI in summer of 2001, 2006, 2011, 2016, and 2020.



325
326

Fig. 8. LISA maps of RSEI in summer of 2001, 2006, 2011, 2016, and 2020.

327 **4. Discussion**

328 The existing studies mainly utilized the same period images in different years to construct the
 329 RSEI to assess the temporal and spatial variation of EEQ (Gou and Zhao, 2020; Ji et al., 2020b;
 330 Yuan et al., 2021), which mainly considered the inter-annual variation of EEQ in a specific period.
 331 However, there is no explanation for why images from a specific time period were used to construct
 332 the RSEI to evaluate the EEQ. We synthesized seasonal images to construct RSEI to evaluate EEQ
 333 in the JJJ region in this study, which not only considered the interannual variation of EEQ in the
 334 same season, but also explored the stability of EEQ in the same season under long-term time series.

335 The results revealed that the characteristics of the four indicators were primarily concentrated
 336 on the PC1, particularly in the summer. Besides, the greenness (NDVI) and wetness (WET) indica-
 337 tors of PC1 had positive effects on EEQ, while heat (LST) and dryness (NDBSI) indicators were
 338 negative, respectively (Table. 2). The proved results were similar to the previous researches (Huang
 339 et al., 2021; Ji et al., 2022; Yuan et al., 2021).

340 However, the Pearson correlation coefficient between seasonal RSEI and the four indicators
 341 showed a great difference in different seasons (Table. 4). Seasonal RSEI was positively correlated
 342 with NDVI and WET, but negatively with NDBSI. Meanwhile, the correlation between LST and
 343 RSEI was sometimes positive or negative. Furthermore, previous studies on RSEI time series have
 344 typically used a specific period to assess the changing characteristics of RSEI. Instance, some re-
 345 searchers chose the image of the growing season (July to September, 1 June to 31 October, and May
 346 to October) to construct RSEI (Cao et al., 2022; Ji et al., 2020b; Jian et al., 2022). But there is no
 347 explanation for chose the images of the above period. Fortunately, the correlation signs between the
 348 four indicators and summer RSEI showed consistency in different years (NDVI, WET are positive,
 349 and LST, NDBSI are negative). All the correlation coefficients in summer showed moderate corre-
 350 lation (abs: 0.4 - 0.6), strong correlation (abs: 0.6 - 0.8), and high correlation (abs: 0.8 - 1) (Table.
 351 4). This can be explained by that vegetation greenness is a key factor for RSEI (Xu and Deng, 2022),
 352 and vegetation grows the most flourish and greenest in summer, while the leaves turn yellow in
 353 autumn and fall off in spring winter. In addition, to explore the correlation between the four indica-
 354 tors and RSEI in different seasons, we plotted the standard deviation and the mean of the correlation
 355 coefficients in different seasons from 2001 to 2020 (Fig. 9). The results showed that the standard
 356 deviation of the correlation between the four indicators and RSEI fluctuated slightly in summer,
 357 which the std of NDVI, WET, LST, and, NDBSI were 0.005, 0.052, 0.026, and 0.017, respectively.

358 **Table 4**

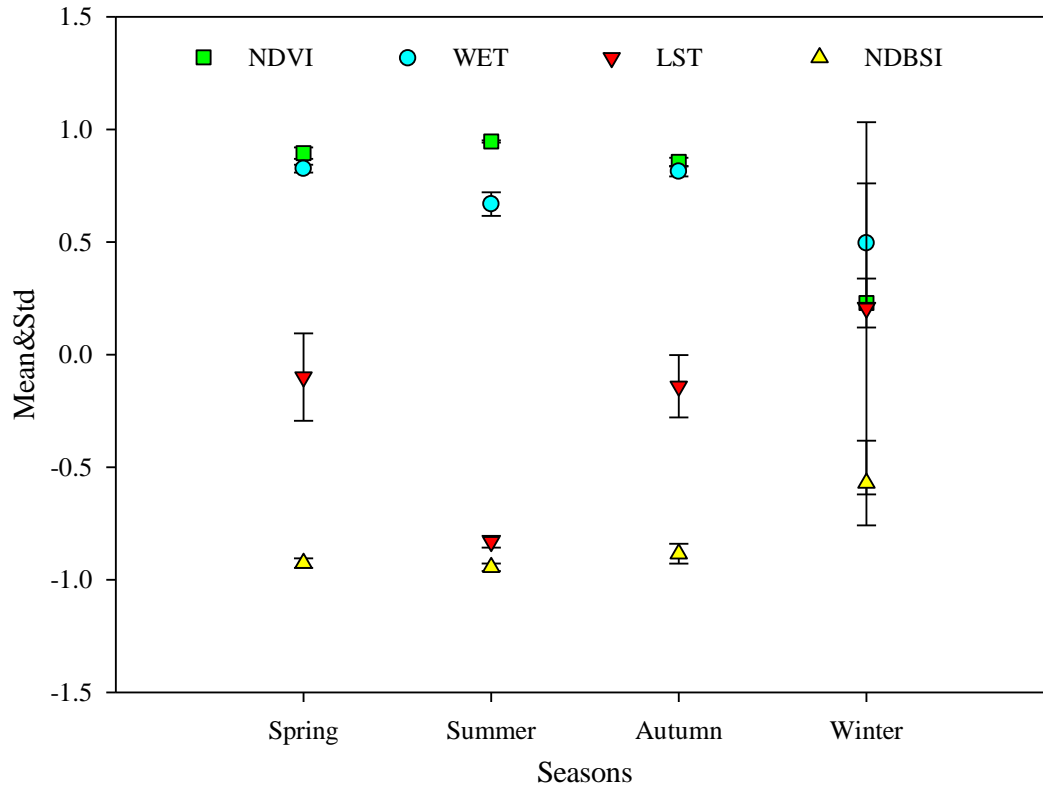
359 Pearson correlation analysis of seasonal RSEI with four indicators.

Years	Indicators	Spring/ ρ	Summer/ ρ	Autumn/ ρ	Winter/ ρ
2001	NDVI	0.884**	0.941**	0.834**	0.161**
	WET	0.826**	0.755**	0.824**	0.416**
	LST	-0.415**	-0.842**	-0.027**	0.873**
	NDBSI	-0.917**	-0.962**	-0.913**	-0.767**
2006	NDVI	0.853**	0.953**	0.837**	0.284**
	WET	0.798**	0.677**	0.826**	0.445**
	LST	0.180**	-0.854**	-0.218**	0.790**
	NDBSI	-0.953**	-0.952**	-0.890**	-0.751**
2011	NDVI	0.897**	0.949**	0.859**	0.0667**
	WET	0.822**	0.591**	0.779**	0.065**
	LST	-0.171**	-0.837**	0.032**	0.970**
	NDBSI	-0.890**	-0.941**	-0.944**	-0.498**
2016	NDVI	0.919**	0.950**	0.880**	0.386**
	WET	0.832**	0.665**	0.799**	0.787**
	LST	-0.046**	-0.842**	-0.358**	-0.718**
	NDBSI	-0.936**	-0.953**	-0.817**	-0.581**
2020	NDVI	0.922**	0.941**	0.871**	0.250**
	WET	0.852**	0.656**	0.841**	0.765**

LST	-0.046**	-0.780**	-0.131**	-0.886**
NDBSI	-0.933**	-0.914**	-0.856**	-0.254**

360 **Note: ** denotes at level 0.01 (double-tailed), with significant correlation**

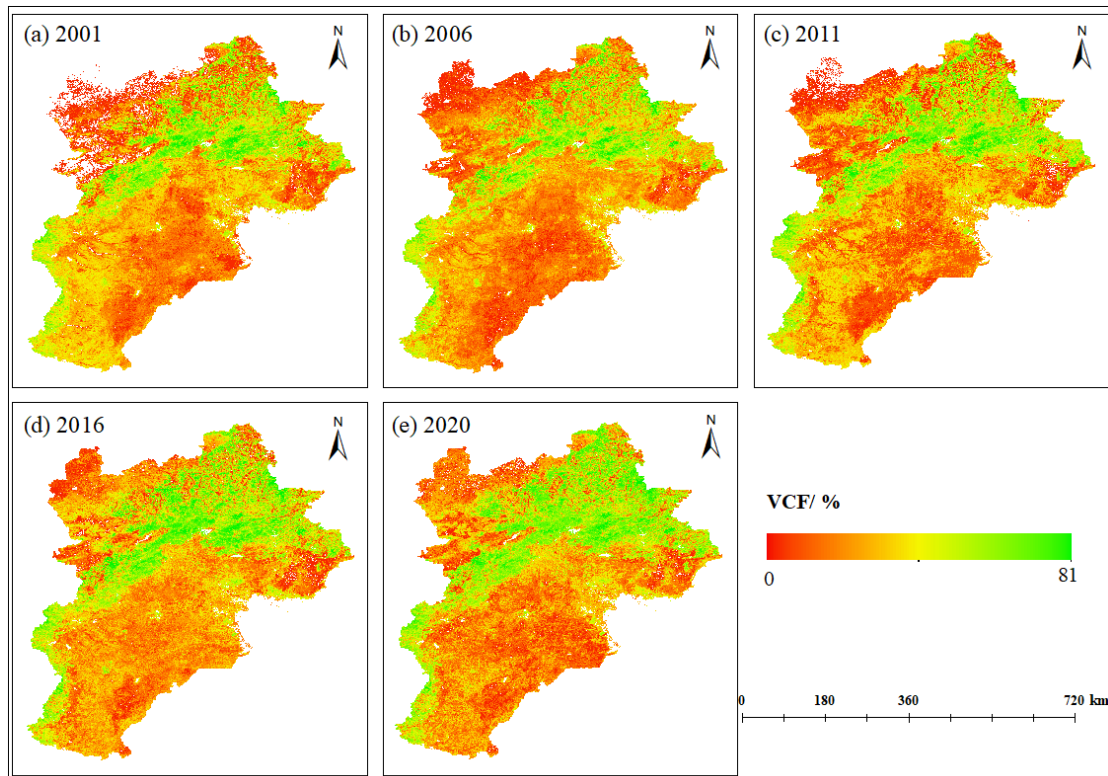
361 However, the changes intensities of RSEI of different levels in the same season of adjacent
362 years were relatively slightly (the scores are mainly -1, 0 and 1) (Fig. 6). Land use types, climate
363 change, and human intervention may all be closely related to this (Yuan et al., 2021). Therefore, the
364 spatiotemporal distribution of different levels of RSEI was significantly different in seasons (Fig.
365 5).



366 **Fig. 9.** The mean and standard deviation of correlation coefficients between RSEI and the four in-
367 dicators in different seasons.
368

369 In order to determine the optimal season to construct RSEI for ecological quality assessment,
370 we used VCF to compare with RSEI of different seasons. The percent tree cover showed a con-
371 sistent spatial distribution in the JJJ region from 2001 to 2020, and the VCF from the western edge
372 to the central region and the northeast (Chengde City) is significantly higher than other regions
373 (Fig. 10). By comparing the spatial distribution changes of the four seasonal RSEI and VCF under
374 the long time series, we found that the spatial distribution of RSEI was consistent with that of
375 VCF only summer. (see Fig. 5). The distribution of RSEI and VCF in the other three seasons
376 showed great differences. Moreover, previous studies have shown that the improvement of ecolog-
377 ical environment quality is related to the increase of vegetation cover, and the destruction of vege-
378 tation cover will lead to a rapid decline in ecological quality(Cheng and He, 2019; Su et al.,
379 2022).

380
381
382



383

384

Fig. 10. The spatial distribution of Vegetation Continuous Fields (VCF) of JJJ region from 2001 to 2020.

385

386

387

4.1. Limitation

388

389

390

391

392

393

394

395

396

397

398

399

400

401

402

403

404

405

406

407

Although this study analyzed the stability of seasonal RSEI in a long time series and reveals the spatio-temporal variation of seasonal EEQ of the JJJ region and proved that the summer is the most suitable time to conduct RSEI, it has several limitations. 1) the traditional RSEI was employed that integrated by NDVI, WET, LST, and NDBSI indicators to assess the changes of EEQ in the JJJ metropolitan region in this study. However, on the basis of the traditional four indicators, some researchers add the factors such as GDP, population, and aerosol optical depth to conduct the MRSEI (Nong et al., 2021; Zhang et al., 2023). 2) We chose MODIS and its product data to calculate RSEI due to the large-scale study area and the long time series study period, but the fine temporospatial changes of EEQ of the coarse-resolution of 500m are difficult to capture. However, the acquisition of the high-precision and multi-temporal used for EEQ analysis is time-consuming and labour-intensive (Huang et al., 2021). Therefore, how to improve the computing power and use multi-temporal and high spatial resolution images (such as Landsat and Sentinel-2) to evaluate EEQ changes in large-scale research areas is an important direction to be studied in the future. 3) The study focuses on the temporospatial evolution of seasonal RSEI. The vast majority bad observations in northern Zhangjiakou and Chengde City despite the synthesis of 3-month images in winter (Fig. 3). Although we employed linear interpolation method for compensate the bad observations, the interpolation results are still abnormal due to the lack of good observation for three months or longer for the pixels (Fig. 6n, 6x). In the reconstruction of long-term continuous missing values in Landsat NDVI time series, the Gap Filling and Savitzky-Golay (GF-SG) method performed best (Chen et al., 2021b), which can be used to reconstruct the bad observations in future research. 4) Chen et al.

408 (2021a) adopted different synthesis methods (median, max, min, mean) to synthesize the images of
409 the rubber forest disaster before and after the tornado, and proved that the images synthesized by
410 different synthesis methods in different periods have significant differences. In this study, the me-
411 dian function is taken for seasonal image synthesis and constructed RSEI to assess the EEQ of the
412 JJJ region. The influence by using mean, max, or min functions for seasonal image synthesis for
413 RSEI needs further study.

414 **5. Conclusions**

415 Since the RSEI is completely based on remote sensing, the weights of each index are objectively
416 determined from the load values generated by the principal component transformation, and there is
417 no artificial subjective weighting, it is proved that the model has strong robustness. The results
418 showed that the eigenvalues contribution rate of PC1 was more than 71% in the summer, while the
419 other seasons ranged from 40.157% to 60.707%. In addition, the fluctuation of RSEI in the summer
420 from 2001 to 2020 was 0.428, 0.480, 0.505, 0.481, and 0.590, respectively, which indicated that the
421 EEQ of the JJJ has improved in this period. The EEQ in the northeast of the study area was much
422 better than that in other places in the summer, which is consistent with the spatial distribution of
423 VCF. There were significant disparities in the changes of EEQ in the JJJ region across different
424 seasons. Furthermore, the change intensities were relatively low, focusing primarily on the scores -
425 1, 0, and 1. LULC and climate change may explain the variation of EEQ in the JJJ region. RSEI
426 was significantly correlated with the other four indicators and was relatively stable in summer. The
427 findings of this study suggest that the summer images should be employed as much as possible when
428 evaluate the EEQ of urban agglomeration to ensure the veracity of the calculation results of RSEI
429 and the objectivity of ecological quality assessment.

430 **CRedit authorship contribution statement**

431 **Shaodong Huang:** contributed ideas and designed the study, collected the remote sensing data
432 including the MODIS and its product data, built the algorithm based on GEE, conducted the data
433 analysis, and wrote the manuscript, which all above done with support from the help of all the other
434 authors and all authors gave final approval for publication. **Yujie Li:** data analysis and mapping.
435 **Haowen Hu:** data collected and export to local. **Pengcheng Xue:** data analysis and produced tables.
436 **Nina Xiong:** contributed ideas, designed the study, and wrote the manuscript. **Jia Wang:** contrib-
437 uted ideas, designed the study, conducted the data analysis, and wrote the manuscript with the help
438 of all the other authors.

439

440 **Declaration of competing interest**

441 The authors declare that they have no known competing financial interests or personal relation-
442 ships that could have appeared to influence the work reported in this paper.

443 **Acknowledgments**

444 This work was supported by the Fundamental Research Funds for the Beijing Natural Science
445 Foundation Program (grant number 8222069, 8222052); the Natural Science Foundation of China
446 (grant numbers 42071342, 42101473, 42171329), and thank the editors and anonymous reviewers
447 for their kindly view and constructive suggestions.

448 **References**

- 449 Ahlgren, P., Jarneving, B. and Rousseau, R., 2003. Requirements for a cocitation similarity measure,
 450 with special reference to Pearson's correlation coefficient. *Journal of the American Society for*
 451 *Information Science and Technology*, 54(6): 550-560.
- 452 Airiken, M., Zhang, F., Chan, N.W. and Kung, H.T., 2022. Assessment of spatial and temporal ecological
 453 environment quality under land use change of urban agglomeration in the North Slope of
 454 Tianshan, China. *Environ Sci Pollut Res Int*, 29(8): 12282-12299.
- 455 Anselin, L., 1995. Local indicators of spatial association—LISA. *Geographical analysis*, 27(2): 93-115.
- 456 Cao, J., Wu, E., Wu, S., Fan, R., Xu, L., Ning, K., Li, Y., Lu, R., Xu, X. and Zhang, J., 2022.
 457 Spatiotemporal Dynamics of Ecological Condition in Qinghai-Tibet Plateau Based on Remotely
 458 Sensed Ecological Index. *Remote Sensing*, 14(17): 4234.
- 459 Chen, B., Yun, T., An, F. and Kou, W., 2021a. Assessment of tornado disaster in rubber plantation in
 460 western Hainan using Landsat and Sentinel-2 time series images. *National Remote Sensing*
 461 *Bulletin*, 25(3): 816-829 (in Chinese).
- 462 Chen, Y., Cao, R., Chen, J., Liu, L. and Matsushita, B., 2021b. A practical approach to reconstruct high-
 463 quality Landsat NDVI time-series data by gap filling and the Savitzky–Golay filter. *ISPRS*
 464 *Journal of Photogrammetry and Remote Sensing*, 180: 174-190.
- 465 Cheng, Z. and He, Q., 2019. Remote Sensing Evaluation of the Ecological Environment of Su-Xi-Chang
 466 City Group based on Remote Sensing Ecological Index (RSEI). *Remote Sensing Technology*
 467 *and Application*, 34(3): 531-539 (in Chinese).
- 468 Deng, Y., Ling, Z., Sun, N. and LV, J., 2021. Daily Estimation of Soil Moisture over Beijing-Tianjin-
 469 Hebei Region based on General Regression Neural Network Model. *Journal of Geo-information*
 470 *Science*, 23(04): 749-761 (In Chinese).
- 471 Gao, P., Kasimu, A., Zhao, Y., Lin, B., Chai, J., Ruzi, T. and Zhao, H., 2020. Evaluation of the Temporal
 472 and Spatial Changes of Ecological Quality in the Hami Oasis Based on RSEI. *Sustainability*,
 473 12(18): 7716.
- 474 Gong, J., Xie, Y., Zhao, C. and Gao, Y., 2014. Landscape ecological risk assessment and spatial and
 475 temporal differentiation of Bailong River Basin in Gansu Province. *China Environ. Sci*, 34:
 476 2153-2160.
- 477 Gorelick, N., Hancher, M., Dixon, M., Ilyushchenko, S., Thau, D. and Moore, R., 2017. Google Earth
 478 Engine: Planetary-scale geospatial analysis for everyone. *Remote sensing of Environment*, 202:
 479 18-27.
- 480 Gou, R. and Zhao, J., 2020. Eco-Environmental Quality Monitoring in Beijing, China, Using an RSEI-
 481 Based Approach Combined With Random Forest Algorithms. *IEEE Access*, 8: 196657-196666.
- 482 Han, N., Hu, K., Yu, M., Jia, P. and Zhang, Y., 2022. Incorporating Ecological Constraints into the
 483 Simulations of Tropical Urban Growth Boundaries: A Case Study of Sanya City on Hainan
 484 Island, China. *Applied Sciences*, 12(13): 6409.
- 485 Hang, X., Luo, X., Cao, Y. and Li, Y., 2020. Ecological quality assessment and the impact of urbanization
 486 based on RSEI model for Nanjing, Jiangsu Province, China. *Ying Yong Sheng tai xue bao= The*
 487 *Journal of Applied Ecology*, 31(1): 219-229.
- 488 Hu, X. and Xu, H., 2018. A new remote sensing index for assessing the spatial heterogeneity in urban
 489 ecological quality: A case from Fuzhou City, China. *Ecological Indicators*, 89: 11-21.
- 490 Huang, H., Chen, W., Zhang, Y., Qiao, L. and Du, Y., 2021. Analysis of ecological quality in Lhasa
 491 Metropolitan Area during 1990–2017 based on remote sensing and Google Earth Engine

492 platform. *Journal of Geographical Sciences*, 31(2): 265-280.

493 Hui, J., Bai, Z. and Ye, B., 2021. Eco-Environment Evaluation of Grassland Based on Remote Sensing
494 Ecological Index: A Case in Hulunbuir Area, China. *Journal of Computer and Communications*,
495 9(6): 203-213.

496 Jeong, A. and Dorn, R.I., 2019. Soil erosion from urbanization processes in the Sonoran Desert, Arizona,
497 USA. *Land Degradation & Development*, 30(2): 226-238.

498 Ji, J., Tang, Z., Zhang, W., Liu, W., Jin, B., Xi, X., Wang, F., Zhang, R., Guo, B., Xu, Z., Shifaw, E.,
499 Xiong, Y., Wang, J., Xu, S. and Wang, Z., 2022. Spatiotemporal and Multiscale Analysis of the
500 Coupling Coordination Degree between Economic Development Equality and Eco-
501 Environmental Quality in China from 2001 to 2020. *Remote Sensing*, 14(3): 737.

502 Ji, J., Wang, S., Zhou, Y., Liu, W. and Wang, L., 2020a. Spatiotemporal Change and Landscape Pattern
503 Variation of Eco-Environmental Quality in Jing-Jin-Ji Urban Agglomeration From 2001 to 2015.
504 *IEEE Access*, 8: 125534-125548.

505 Ji, J., Wang, S., Zhou, Y., Liu, W. and Wang, L., 2020b. Studying the Eco-Environmental Quality
506 Variations of Jing-Jin-Ji Urban Agglomeration and Its Driving Factors in Different Ecosystem
507 Service Regions From 2001 to 2015. *IEEE Access*, 8: 154940-154952.

508 Ji, J., Wang, S., Zhou, Y., Liu, W. and Wang, L., 2021. Studying the coupling coordination degree between
509 socio-economic and eco-environment of Jing-Jin-Ji urban agglomeration during 2001-2015.
510 *IOP Conference Series: Earth and Environmental Science*, 675(1): 012043.

511 Jian, K., Wang, S., Wu, X. and Zhang, Q., 2022. Analysis of the Eco-environmental Quality Index in the
512 Tropical Rainforest National Park in China during 1990-2020.

513 Jing, Y., Zhang, F., He, Y., Kung, H.-t., Johnson, V.C. and Arikena, M., 2020. Assessment of spatial and
514 temporal variation of ecological environment quality in Ebinur Lake Wetland National Nature
515 Reserve, Xinjiang, China. *Ecological Indicators*, 110: 105874.

516 Kalantari, Z., Ferreira, C.S.S., Walsh, R.P.D., Ferreira, A.J.D. and Destouni, G., 2017. Urbanization
517 development under climate change: Hydrological responses in a peri-urban Mediterranean
518 catchment. *Land degradation & development*, 28(7): 2207-2221.

519 Levin, N., Kyba, C.C., Zhang, Q., de Miguel, A.S., Román, M.O., Li, X., Portnov, B.A., Molthan, A.L.,
520 Jechow, A. and Miller, S.D., 2020. Remote sensing of night lights: A review and an outlook for
521 the future. *Remote Sensing of Environment*, 237: 111443.

522 Li, Y., Chen, M. and Fu, Y., 2022. Analysis of the changes in the Beijing-Tianjin-Hebei urban
523 agglomeration's spatial structure using NPP-VIIRS data. *Bulletin of Surveying and
524 Mapping*(02): 50-55 (in Chinese).

525 Liang, Y., Zou, B., Feng, H. and Liu, N., 2022. Seasonal deviation correction enhanced BGIM
526 downscaling algorithm for remote sensing AOD products. *National Remote Sensing Bulletin*,
527 26(08): 1602-1613 (in Chinese).

528 Liao, W. and Jiang, W., 2020. Evaluation of the Spatiotemporal Variations in the Eco-environmental
529 Quality in China Based on the Remote Sensing Ecological Index, *Remote Sensing*.

530 Liao, W., Jiang, W. and Huang, Z., 2022. Spatiotemporal variations of eco-environment in the Guangxi
531 Beibu Gulf Economic Zone based on remote sensing ecological index and granular computing.
532 *Journal of Geographical Sciences*, 32(9): 1813-1830.

533 Liu, C., Yang, M., Hou, Y., Zhao, Y. and Xue, X., 2021. Spatiotemporal evolution of island ecological
534 quality under different urban densities: A comparative analysis of Xiamen and Kinmen Islands,
535 southeast China. *Ecological Indicators*, 124: 107438.

536 Liu, X.Y., Zhang, X.X., He, Y.R. and Luan, H.J., 2020. Monitoring and Assessment of Ecological Change
537 in Coastal Cities Based on RseI. *The International Archives of the Photogrammetry, Remote*
538 *Sensing and Spatial Information Sciences*, XLII-3/W10: 461-470.

539 Lobser, S. and Cohen, W., 2007. MODIS tasselled cap: land cover characteristics expressed through
540 transformed MODIS data. *International Journal of Remote Sensing*, 28(22): 5079-5101.

541 Maity, S., Das, S., Pattanayak, J.M., Bera, B. and Shit, P.K., 2022. Assessment of ecological environment
542 quality in Kolkata urban agglomeration, India. *Urban Ecosystems*: 1-18.

543 McDonald, R.I., Marcotullio, P.J. and Güneralp, B., 2013. Urbanization and global trends in biodiversity
544 and ecosystem services, *Urbanization, biodiversity and ecosystem services: Challenges and*
545 *opportunities*. Springer, Dordrecht, pp. 31-52.

546 Mutanga, O. and Kumar, L., 2019. Google earth engine applications. *MDPI*, pp. 591.

547 Nong, L., WANG, J. and YU, Y., 2021. Research on Ecological Environment Quality in Central Yunnan
548 Based on MRSEI Model. *Journal of Ecology and Rural Environment*, 37(8): 972-982 (in
549 Chinese).

550 Rousel, J., Haas, R., Schell, J. and Deering, D., 1973. Monitoring vegetation systems in the great plains
551 with ERTS, *Proceedings of the Third Earth Resources Technology Satellite—1 Symposium*;
552 *NASA SP-351*, pp. 309-317.

553 Schneider, A., Mertes, C.M., Tatem, A., Tan, B., Sulla-Menashe, D., Graves, S., Patel, N., Horton, J.A.,
554 Gaughan, A. and Rollo, J.T., 2015. A new urban landscape in East–Southeast Asia, 2000–2010.
555 *Environmental Research Letters*, 10(3): 034002.

556 Stöckli, R., Vermote, E., Saleous, N., Simmon, R. and Herring, D., 2005. The Blue Marble Next
557 Generation-A true color earth dataset including seasonal dynamics from MODIS. Published by
558 the NASA Earth Observatory.

559 Su, S., Zhaoning, G., Wenjing, Z., Yuan, Z. and Yifei, W., 2022. Change of vegetation coverage
560 and assessment of ecological environment quality in Beiyun River Basin. *Acta Scientiae*
561 *Circumstantiae*, 42(1): 19-27 (in Chinese).

562 Sun, C., Li, X., Zhang, W. and Li, X., 2020. Evolution of ecological security in the tableland region of
563 the Chinese loess plateau using a remote-sensing-based index. *Sustainability*, 12(8): 3489.

564 Tamiminia, H., Salehi, B., Mahdianpari, M., Quackenbush, L., Adeli, S. and Brisco, B., 2020. Google
565 Earth Engine for geo-big data applications: A meta-analysis and systematic review. *ISPRS*
566 *Journal of Photogrammetry and Remote Sensing*, 164: 152-170.

567 Tian, Y., Zhou, D. and Jiang, G., 2020. Conflict or Coordination? Multiscale assessment of the spatio-
568 temporal coupling relationship between urbanization and ecosystem services: The case of the
569 Jingjinji Region, China. *Ecological Indicators*, 117: 106543.

570 Turner, W., Spector, S., Gardiner, N., Fladeland, M., Sterling, E. and Steininger, M., 2003. Remote
571 sensing for biodiversity science and conservation. *Trends in ecology & evolution*, 18(6): 306-
572 314.

573 Vermote, E., Kotchenova, S. and Ray, J., 2011. MODIS surface reflectance user’s guide. MODIS Land
574 Surface Reflectance Science Computing Facility, version, 1: 1-40.

575 Wan, Z., Hook, S. and Hulley, G., 2015. MOD11A2 MODIS/Terra land surface temperature/emissivity8-
576 day L3 global 1 km SIN grid V006; distributed by NASA EOSDIS LP DAAC. USGS, Sioux
577 Falls.

578 Wang, H., Jia, G., Fu, C., Feng, J., Zhao, T. and Ma, Z., 2010. Deriving maximal light use efficiency
579 from coordinated flux measurements and satellite data for regional gross primary production

580 modeling. *Remote Sensing of Environment*, 114(10): 2248-2258.

581 Wang, J., Xiao, X., Qin, Y., Dong, J., Geissler, G., Zhang, G., Cejda, N., Alikhani, B. and Doughty, R.B.,
582 2017. Mapping the dynamics of eastern redcedar encroachment into grasslands during 1984–
583 2010 through PALSAR and time series Landsat images. *Remote Sensing of Environment*, 190:
584 233-246.

585 Wang, S., Zhang, X., Zhu, T., Yang, W. and Zhao, J., 2016. Assessment of ecological environment quality
586 in the Changbai Mountain Nature Reserve based on remote sensing technology. *Progress in*
587 *Geography*, 35(10): 1269.

588 Wen, L., Dong, S., Li, Y., Li, X., Shi, J., Wang, Y., Liu, D. and Ma, Y., 2013. Effect of degradation
589 intensity on grassland ecosystem services in the alpine region of Qinghai-Tibetan Plateau, China.
590 *PloS one*, 8(3): e58432.

591 Wu, T., Sang, S., Wang, S., Yang, Y. and Li, M., 2020. Remote sensing assessment and spatiotemporal
592 variations analysis of ecological carrying capacity in the Aral Sea Basin. *Sci Total Environ*, 735:
593 139562.

594 Xia, Q., Chen, Y., Zhang, X. and Ding, J., 2022. Spatiotemporal Changes in Ecological Quality and Its
595 Associated Driving Factors in Central Asia. *Remote Sensing*, 14(14): 3500.

596 Xiong, Y., Xu, W., Lu, N., Huang, S., Wu, C., Wang, L., Dai, F. and Kou, W., 2021. Assessment of spatial–
597 temporal changes of ecological environment quality based on RSEI and GEE: A case study in
598 Erhai Lake Basin, Yunnan province, China. *Ecological Indicators*, 125: 107518.

599 Xu, H., 2013. A remote sensing index for assessment of regional ecological changes. *China*
600 *Environmental Science*, 33(5): 889-897 (in Chinese).

601 Xu, H. and Deng, W., 2022. Rationality Analysis of MRSEI and Its Difference with RSEI. *Remote*
602 *Sensing Technology and Application*, 37(01): 1-7 (in Chinese).

603 Xu, H., Wang, M., Shi, T., Guan, H., Fang, C. and Lin, Z., 2018. Prediction of ecological effects of
604 potential population and impervious surface increases using a remote sensing based ecological
605 index (RSEI). *Ecological Indicators*, 93: 730-740.

606 Xu, H., Wang, Y., Guan, H., Shi, T. and Hu, X., 2019. Detecting Ecological Changes with a Remote
607 Sensing Based Ecological Index (RSEI) Produced Time Series and Change Vector Analysis.
608 *Remote Sensing*, 11(20): 2345.

609 Yang, X., Meng, F., Fu, P., Wang, Y. and Liu, Y., 2022. Time-frequency optimization of RSEI: A case
610 study of Yangtze River Basin. *Ecological Indicators*, 141: 109080.

611 Yang, X., Meng, F., Fu, P., Zhang, Y. and Liu, Y., 2021. Spatiotemporal change and driving factors of the
612 Eco-Environment quality in the Yangtze River Basin from 2001 to 2019. *Ecological Indicators*,
613 131: 108214.

614 Yuan, B., Fu, L., Zou, Y., Zhang, S., Chen, X., Li, F., Deng, Z. and Xie, Y., 2021. Spatiotemporal change
615 detection of ecological quality and the associated affecting factors in Dongting Lake Basin,
616 based on RSEI. *Journal of Cleaner Production*, 302: 126995.

617 Yue, H., Liu, Y., Li, Y. and Lu, Y., 2019. Eco-environmental quality assessment in China’s 35 major cities
618 based on remote sensing ecological index. *Ieee Access*, 7: 51295-51311.

619 Zang, S., Wu, C., Liu, H. and Na, X., 2011. Impact of urbanization on natural ecosystem service values:
620 a comparative study. *Environmental monitoring and assessment*, 179(1): 575-588.

621 Zhang, C.-L., Li, Q., Shen, Y.-P., Zhou, N., Wang, X.-S., Li, J. and Jia, W.-R., 2018. Monitoring of aeolian
622 desertification on the Qinghai-Tibet Plateau from the 1970s to 2015 using Landsat images.
623 *Science of The Total Environment*, 619-620: 1648-1659.

624 Zhang, J., YANG, L., Gong, E., Yu, W., Ren, J. and Liu, M., 2023. Dynamic monitoring of eco-
625 environment quality in Xi' an based on GEE and adjusted RSEI. *Acta Ecologica*
626 *Sinica*(05): 1-14 (in Chinese).

627 Zhang, P., Liu, S., Zhao, Z., Liu, C., Xu, L. and Gao, X., 2021a. Supply and demand measurement and
628 spatio-temporal evolution of ecosystem services in Beijing-Tianjin-Hebie Region. *Acta*
629 *Ecologica Sinica*, 41(09): 3354-3367 (in Chinese).

630 Zhang, Q., Sun, C., Chen, Y., Chen, W., Xiang, Y., Li, J. and Liu, Y., 2022. Recent Oasis Dynamics and
631 Ecological Security in the Tarim River Basin, Central Asia. *Sustainability*, 14(6): 3372.

632 Zhang, T., Yang, R., Yang, Y., Li, L. and Chen, L., 2021b. Assessing the Urban Eco-Environmental
633 Quality by the Remote-Sensing Ecological Index: Application to Tianjin, North China. *ISPRS*
634 *International Journal of Geo-Information*, 10(7): 475.

635 Zhou, D., Tian, Y. and Jiang, G., 2018. Spatio-temporal investigation of the interactive relationship
636 between urbanization and ecosystem services: Case study of the Jingjinji urban agglomeration,
637 China. *Ecological Indicators*, 95: 152-164.

638 Zhou, J. and Liu, W., 2022. Monitoring and Evaluation of Eco-Environment Quality Based on Remote
639 Sensing-Based Ecological Index (RSEI) in Taihu Lake Basin, China. *Sustainability*, 14(9): 5642.

640 Zhu, D., Chen, T., Zhen, N. and Niu, R., 2020. Monitoring the effects of open-pit mining on the eco-
641 environment using a moving window-based remote sensing ecological index. *Environmental*
642 *Science and Pollution Research*, 27(13): 15716-15728.

643 Zhu, Z. and Woodcock, C.E., 2012. Object-based cloud and cloud shadow detection in Landsat imagery.
644 *Remote Sensing of Environment*, 118: 83-94.

645